Results from Ground-based Monitoring of Spectral Aerosol Optical Thickness and Horizontal Extinction: Some Specific Characteristics of Dusty Sahelian Atmospheres

A. BEN MOHAMED AND J.-P. FRANGI

Université de Niamey, Faculté des Sciences, Département de Physique, Niamey, Niger

(Manuscript received 14 December 1985, in final form 26 April 1986)

ABSTRACT

This paper presents results of 14 months of ground-based measurements of spectral aerosol optical thickness and horizontal extinction together with related studies, such as relations between these parameters, meteorological parameters of the surface and upper air, and total mass load and size distributions, as performed in Niamey, Niger, in West African Sahel.

1. Introduction

In a previous paper (Ben Mohamed and Frangi, 1983; hereafter referred to as BMF) we reported on the general behavior of atmospheric humidity and turbidity parameters in West African Sahel as deduced from solar transmission measurements initiated and performed daily in Niamey, Niger, since 1981.

The present paper focuses on the analysis of the data collected from November 1982 through December 1983. This represents a total of 865 solar transmission measurements made daily under cloud-free conditions at 0900, 1200 and 1500 GMT; 330 telephotometric, horizontal, spectral extinction measurements carried out together with solar transmission measurements between 1500 and 1600 GMT; and 75 high-volume air samplings of the total mass concentrations of airborne soil particles.

The size distribution of the particles contributing to extinction is inferred from the measurements of spectral aerosol optical thickness following the method described by King et al. (1978). From the horizontal spectral extinction measurements, the aerosol extinction coefficient is derived, and its relations with the horizontal visibility and the aerosol optical thickness are studied. Visibility observations together with total particulate mass sampling were used to derive the relation between mass concentration and visibility.

We concentrated on relationships between spectral aerosol optical thickness and horizontal extinction during the so-called dry season. At this period of the year, the Sahelian zone is predominantly affected by dust pollution. The experimental data were classified as belonging to the "dry" or "humid" season according to the value of precipitable water (w, in centimeters) deduced from solar transmission measurements in the $\rho\sigma\tau$ band. The limit of $w < 2$ cm for the dry season, and consequently $w \geqslant 2$ cm for the humid season, corresponds well, according to Fig. 1 of BMF, to the transition between the two seasons. This limit determined two sets of data that gave the best correlation between spectral aerosol optical thickness and horizontal extinction.

2. Spectral aerosol optical thickness

Solar transmission measurements were made at 350, 380, 440, 500, 641, 876, 1024 and 1610 nm wavelengths. Table 1 gives the bandwidth ($\Delta\lambda$) of the interference filters together with the calibration relative errors on the extraterrestrial constants during the period of the present study. Calibration utilized a Langley plot of data collected on absolutely cloud-free days in Niamey. Only days (6 within the 14-month period) with approximately constant optical thickness were used to derive the final mean values of the spectral extraterrestrial constants used in the computations.

The spectral aerosol optical thickness τ_a is defined as

$$\tau_{a\lambda} = \tau_{t\lambda} - (\tau_{R\lambda} + \tau_{O_3})$$

where $\tau_{t\lambda}$ is the total spectral optical thickness of the atmosphere as derived from the well-known Lambert–Beer law, $\tau_{R\lambda}$ is the Rayleigh or molecular scattering optical depth (Penndorf, 1957), and τ_{O_3} is the optical depth arising from absorption by the atmospheric ozone, which has been evaluated at 500 and 641 nm, assuming a constant midlatitude concentration (Junge, 1963) and absorption coefficients given by Inn and Tanaka (1959).

Errors in determination of $\tau_{a\lambda}$ were computed according to

$$\Delta\tau_{a\lambda} = \pm\left(\frac{1}{m}\left|\frac{\Delta I_\lambda}{I_\lambda}\right| + \frac{1}{m}\left|\frac{\Delta I_{0\lambda}}{I_{0\lambda}}\right| + \Delta\tau_{O_3}\right)$$

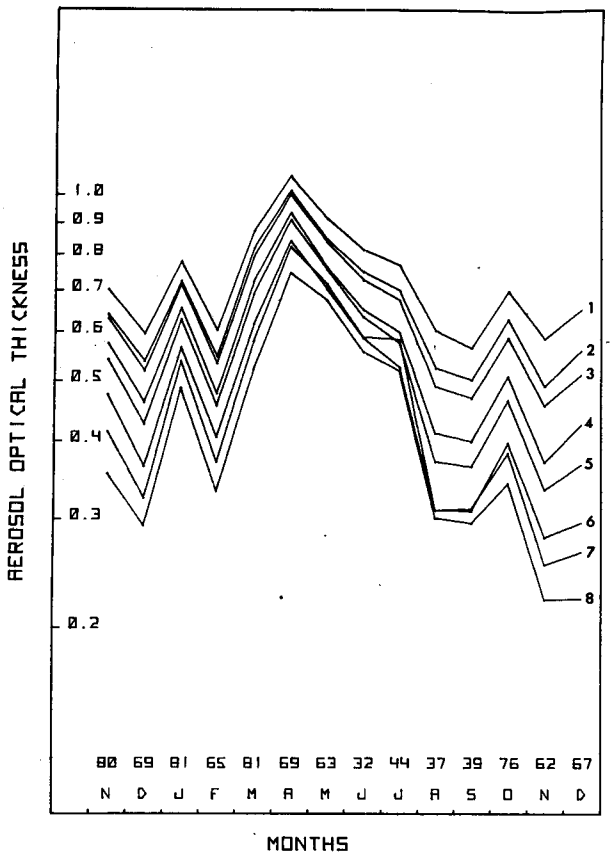

FIG. 1. Geometric mean values of aerosol optical thickness by month at eight wavelengths. The numbers over the abscissa represent the number of measurements per month contributing to each monthly mean. The number to the right of each curve indicates the wavelength, i.e., 1 is 350, 2 is 380, 3 is 440, 4 is 500, 5 is 641, 6 is 876, 7 is 1024 and 8 is 1610 nm.

with $\tau_{a\lambda}$ in the form

$$\tau_{a\lambda} = \frac{\ln \frac{I_{0\lambda}}{I_\lambda S}}{m} - (\tau_{R\lambda} + \tau_{O_3})$$

where

$I_{0\lambda}$ the reading the transmissometer would have outside the atmosphere
I_λ the under-atmosphere reading of the instrument
S a correction factor that depends on solar distance
m the airmass

Assuming a reading error of 1%, minimum and maximum values of $\Delta\tau_{a\lambda}$ for the period under investigation are reported in Table 1. Because the instruments are carried out only when measurements have to be performed, no temperature correction of the data has to be done.

Figure 1 shows the monthly variation of the geometric mean values of aerosol optical thickness at each of the eight wavelengths from November 1982 to December 1983, following the presentation of King et al. (1980) for Tucson, Arizona. The number of measurements per month contributing to each monthly average is indicated by a number over the month on the figure. It is interesting to note, comparing this figure with Fig. 4 of King et al. (1980), that the mean monthly geometric value of spectral aerosol optical thickness at 500 nm at Niamey is nearly ten times that at Tucson, Arizona. One notes in Fig. 1 an increase in $\tau_{a\lambda}$ from February to April (the dry season) and then a corresponding decrease from April to July (the humid season). This is mainly due to an increase in the number of dust events and, consequently, mass loading per event (February–April) and a decrease in the dust mass loading per event (April–September).

3. Horizontal spectral extinction

The measurements of the horizontal spectral extinction coefficient have been made with a telephotometer (Horvath, 1981) equipped with interference filters centered at 499.8 and 645.0 nm with bandwidths of $\Delta\lambda = 50$ and 44 nm, respectively. The instrument consists of an astronomic reflective telescope mounted so that an adjustable stop with a normal size of 1 mm is inserted at the location of the real image of the target, thus defining a small portion of the target to be measured. The light emerging from the stop passes interchangeable interference filters and reaches a photodiode. The photocurrent is proportional to the luminance of the target. A plane-parallel plate, which is inserted in the path of the light, permits the brightness of the target and the horizon to be measured repeatedly without realignment of the telescope.

The measurements were done in cloudless sky conditions only, in order to have a rather uniform illumination along the horizontal path. The instrument was operated on a flat roof at the Department of Physics at the Université de Niamey, approximately 12 m above ground level. The targets, which were rocky hills

TABLE 1. Wavelength and bandwidth of the interference filters, calibration relative errors on the extraterrestrial constants, minimum and maximum values of $\Delta\tau_{a\lambda}$.

λ (nm)	350	380	440	500	641	876	1024	1610
$\Delta\lambda$ (nm)	10	11	12	10	10	17	18	20
$\frac{\Delta I_{0\lambda}}{I_{0\lambda}} 10^2$	6	4	7	2	2	1	2	3
$\Delta\tau_{a\lambda}\, 10^2$	7–19	5–12	7–21	3–8	3–8	2–6	4–8	4–8

at various distances between 1.3 and 12 km, were viewed when they were in their own shadows in order to minimize the errors due to the use of nonblack objects. Corrections for Rayleigh molecular scattering were made on the extinction coefficients using values given under normal conditions by McCartney (1976), thus obtaining the extinction coefficients of the aerosol particles only (b_a). We examined the relationship between the aerosol extinction coefficient, b_a, at wavelength 500 nm and the horizontal visibility. For that purpose we used recorded visibilities at Niamey airport (located approximately 8 km from our measurement site), as well as visibilities estimated according to the Foitsik scheme (Volz, 1980), particularly when visibility was reduced by dust events.

Figure 2 presents the results of 330 measurements; 176 were in the dry season and 154 in the humid season. For the whole dataset, the best fit between the variables b_a at 500 nm and $1/V$ is given by the following regression equation:

$$b_a = \frac{1.45}{V} \tag{1}$$

with a correlation coefficient of $r = 0.96$. Here V is expressed in kilometers and b_a as per kilometer. Curve A of Fig. 2 represents the plot of the function defined by Eq. (1).

Errors of telephotometric measurements of the horizontal spectral extinction coefficient b_a have been discussed by Horvath (1981). In the case of our measurements, the computed relative errors $\Delta b_a/b_a$ at 500 nm vary between 9.8% and 1.5% for visibilities between 1.5 and 30 km, respectively. The Koschmieder formula usually used (curve b) (Middleton, 1968) is also plotted in Fig. 2 between the visual range and the effective atmospheric extinction coefficient along the line of sight, namely, $b_{ext} = 3.9/V$, which is quite different from relation (1) if one considers b_{ext} close to b_a. However, it would be difficult to compare our results with the Koschmieder relation because the Koschmieder theory requires that the atmosphere be illuminated homogeneously, that the object be ideally black and viewed against the horizon, and that the eye of the observer have a constant contrast threshold. Obviously, visibilities estimated at Niamey airport for aviation purposes do not fulfill the above conditions.

4. Relation between spectral aerosol optical thickness and horizontal extinction

We restricted ourselves to the study of the relation between these parameters in the dry season because (i) at that period the extinction is primarily due to suspended airborne soil particles in the air, and (ii) dust events affect significantly large areas over West Africa at the same time. Therefore, the relations derived here can be representative of a large zone, especially when remote sensing over West Africa during the dry season is concerned.

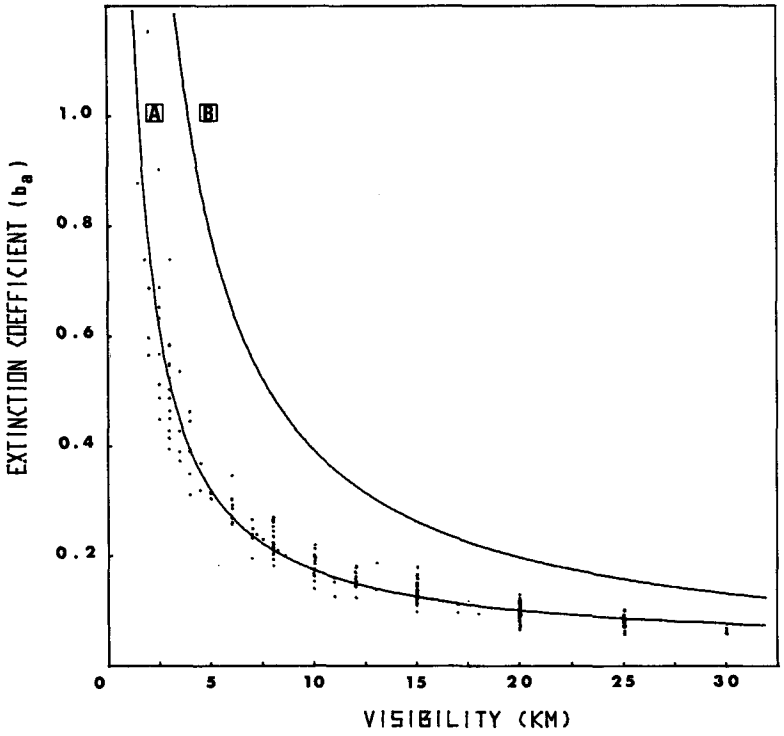

FIG. 2. Curve A: regression curve to the plot of horizontal extinction coefficient at wavelength 500 nm b_a (km^{-1}) vs visibility. Curve B: plot of the Koschmieder relation.

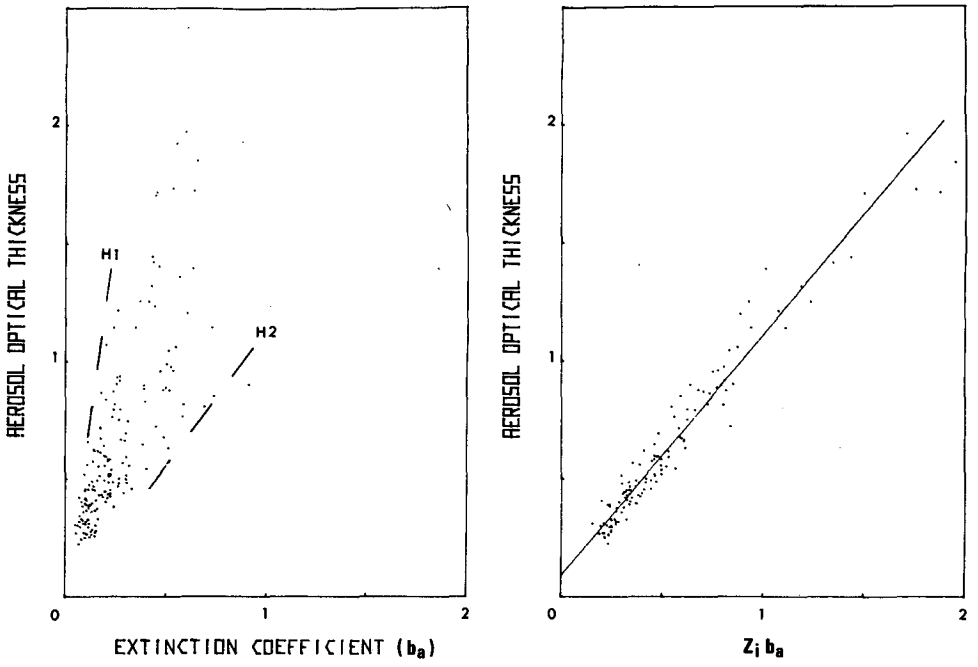

FIG. 3. (a) Plot of aerosol optical thickness τ_a vs horizontal extinction coefficient b_a at 500 nm. (b) Plot of aerosol optical thickness at 500 nm vs dimensionless product $b_{a500}Z_i$ with the corresponding regression line.

Figure 3a presents the plot of data points representing τ_a versus b_a at 500 nm. Obviously, one sees from the scatter of these points that these two parameters are not directly related to each other. Although the data points are scattered, points belonging to the same line passing through the origin are within the equal ratio $\tau_a/b_a = H$—the optical scale height. Thus, H_1 and H_2 in Fig. 3a represent the extreme values of the slopes of the beam of lines originating at 0. In order to physically relate τ_a and b_a at 500 nm, b_a is nondimensionalized by using a convective parameter scale according to the method of parameterization and normalization in the convective boundary layer described by Druilhet et al. (1983). The length scale we used as the empirical length is the thickness of the planetary boundary layer (PBL), Z_i, expressed in kilometers in the text. Experimentally, Z_i is defined as the level at which the first temperature inversion occurs (Deardoff, 1974; Nicholls and Reading, 1979). Thus, comparison of spectral aerosol optical thickness and horizontal extinction suggests the occurrence of an aerosol layer of thickness Z_i.

We selected 131 soundings made during the dry season at 1200 GMT at Niamey airport in such a way that the radiosonde encountered no clouds during its ascent, we determined Z_i, as previously indicated from the plot of potential temperature and mixing ratio vs height. Computations were made for 50 levels from the ground up to the stable layer.

Figure 3b presents the plot of τ_{a500} vs the dimensionless product $b_{a500}Z_i$ and the corresponding regression line. The regression equation obtained from the mathematical fit of the data points is

$$\tau_{a500} = 1.02 Z_i b_{a500} + 0.09 \qquad (2)$$

with a correlation coefficient of $r = 0.97$. An almost identical relationship is obtained at the wavelength 640 nm, with the same correlation. If one defines the ratio $H_a = \tau_a/b_a$ as being the aerosol scale height (Tomasi, 1982; Kaufman and Fraser, 1983), then the relation between H_a and Z_i is given by the following regression equation:

$$H_a = 1.17 Z_i + 0.12 \qquad (3)$$

with a correlation coefficient of $r = 0.93$, H_a and Z_i being expressed in kilometers. As a consequence, horizontal visibility and the spectral aerosol optical thickness will be related through the parameter Z_i. The regression equation between these two quantities from the data points is

$$\tau_{a500} = 1.37 \frac{Z_i}{V} + 0.18 \qquad (4)$$

with a correlation coefficient of $r = 0.90$; V and Z_i are both expressed in kilometers.

The minimum value of τ_a at 500 nm observed in the dataset is $\tau_a = 0.22$. Introducing in Eq. (4) the corresponding $Z_i = 1.25$ km and $V = 30$ km, one ends up with a computed $\tau_{a500} = 0.237$, which agrees well with the observed value. Thus, even in conditions of large surface visibilities, the observed aerosol optical thickness at 500 nm is nonnegligible.

Equations (3) and (4) can be used to estimate the height of a dust layer over the Sahelian region during the dry season since the variation of concentration of dust with height reaches 9% of its ground value at a height of $1.17Z_i$ based on aircraft measurements over Niamey in December 1980 (Durand and Druilhet, 1982).

5. Relation between total mass of airborne particulate matter and visibility

Airborne particulate matter was sampled with a high-volume cascade impactor series 230 from Sierra In struments, Inc., consisting of five stages with rectangular jets and a backup filter. As indicated earlier, the instrument was operated at the same location as the telephotometer. Particulate matter was collected on Weather Measure Corp. glass fiber filters and the instrument was operated at a mean flow rate of 38 ft^3 min^{-1}. The backup filter was changed as soon as the flow rate decreased more than 5%. The sampling time varied from 3 to a maximum of 10 h. A total of 75 samples were collected within the period from December 1982 to April 1983. Mass–visibility relations have been studied by a number of authors (Chepil and Woodruff, 1957; Charlson, 1969; Patterson and Gillette, 1976; Bertrand et al., 1974).

In order to describe our measurements, we used an equation of the form

$$M = \frac{C}{V^{\gamma}} \tag{5}$$

where M is the total mass of airborne soil particles in micrograms per cubic meter, V the estimated visibility in kilometers, and C and γ are determined from the mathematical fit to the data.

The best-fit regression equation between $\log M$ and $\log V$ gives

$$M = \frac{1339.84}{V^{0.67}} \tag{6}$$

with a correlation coefficient of $r = 0.96$. Figure 4 presents the corresponding regression line. Following the comparison between different measurements made by Patterson and Gillette (1976), the value of $\gamma = 0.67$ found in Niamey reflects the increased relative importance of the small particle ($r \leq 10$ μm) mode in the mass distribution, as can be seen later from the plot of impactor data. From Eqs. (4) and (6) one can derive a relation between the aerosol optical thickness at 500 nm and the mass of suspended particulate material which is of the form

$$\tau_{a500} = 2.95 \times 10^{-5} Z_i M^{1.49} + 0.18. \tag{7}$$

For mass samplings made around noontime (PBL fully developed), a comparison between measured and calculated values of aerosol optical thickness at 500 nm shows an agreement within 10% accuracy.

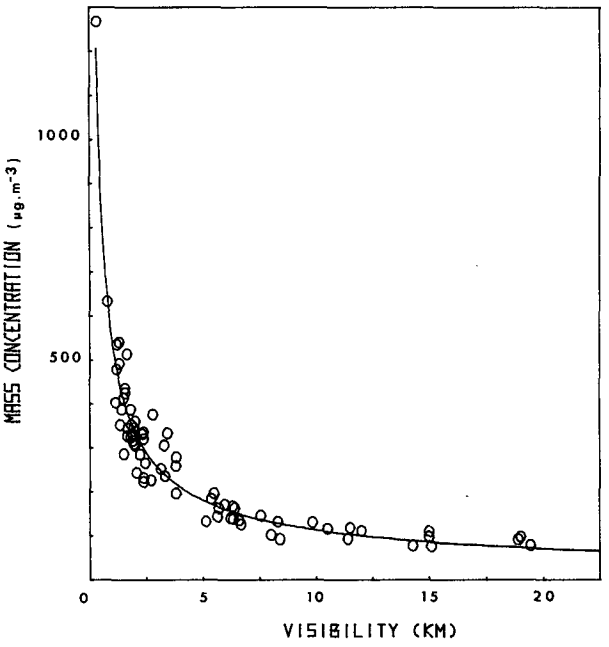

FIG. 4. Plot of total mass concentration vs visibility with the corresponding regression curve.

6. Size distributions of Sahelian aerosols

As stated before, the aerosol size distributions have been derived from the optical thickness data by an inversion method described by King et al. (1978) and King (1982). The Junge (1963) power law,

$$\frac{dN}{d\log r} = Cr^{-v^*}, \tag{8}$$

has been used to describe the size distribution. The exponent v^* in (8) has been shown to be related to the wavelength exponent in the Ångström (1929) empirical relation $\tau_a = \beta\lambda^{-\alpha}$, where β is the extinction coefficient at wavelength $\lambda = 1000$ nm, by a relation of the form $v^* = \alpha + 2$ (Shaw, 1973). In our case, α has been calculated from a least-squares fit to the measured aerosol optical thickness in the 350–1610 nm spectral range. The refractive index used for the computations was that reported by Patterson et al. (1977) for Saharan aerosols, namely, $n = 1.55 - 0.005i$.

Two different meteorological situations illustrated in Figs. 5a, b were selected in order to give an idea of the two extreme situations that can be found in this region when the optical state of the atmosphere is concerned. Figure 5a presents a typical situation of so-called dry haze over West Africa as illustrated by the surface meteorological chart from Niamey Airport at 1200 GMT 10 December 1982. On this chart the Sahelian zone affected by dust pollution is located between the dashed line and the double line representing the intertropical discontinuity (the apparent limit between the dry continental and humid marine air masses).

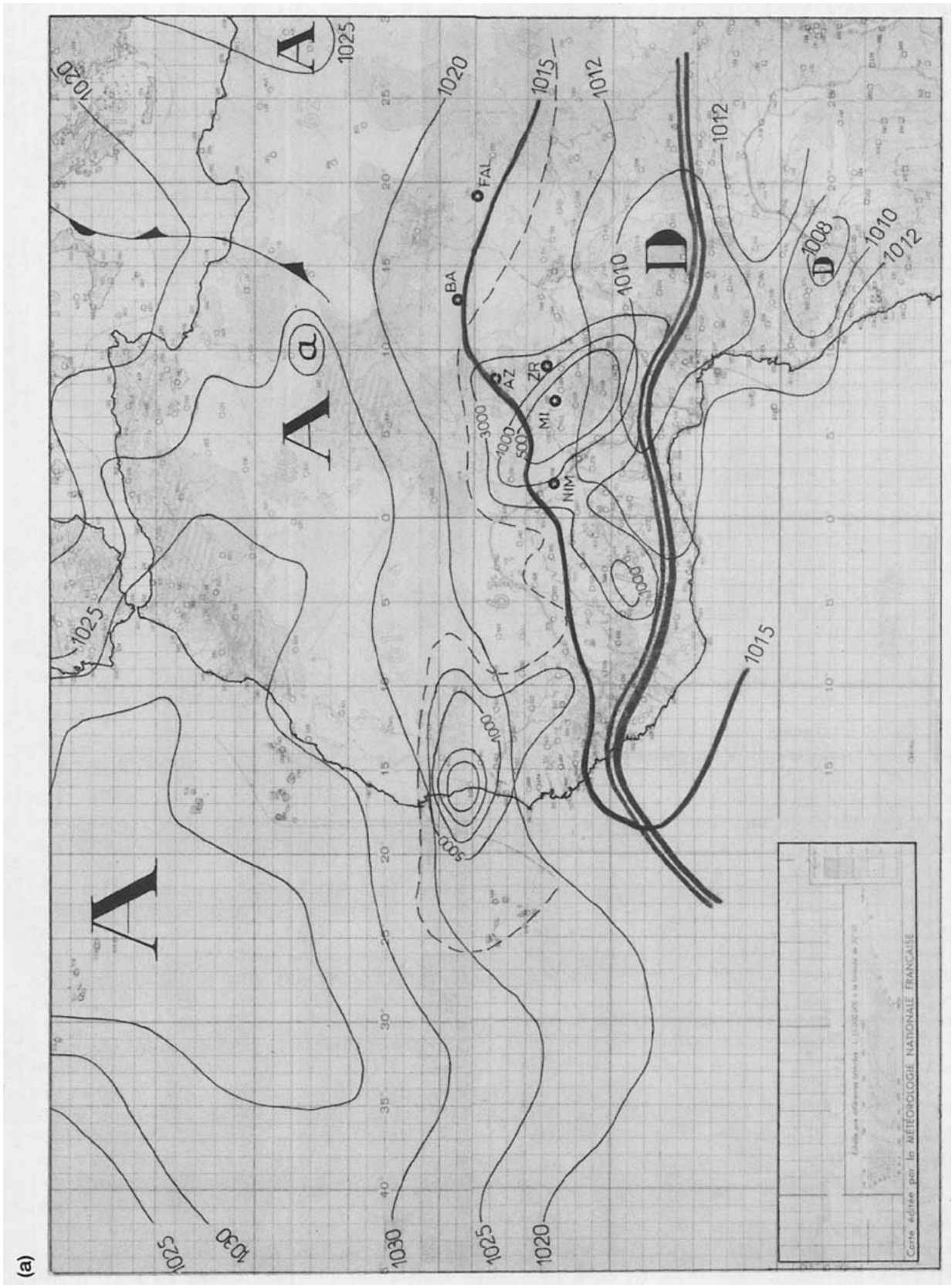

FIG. 5. Surface meteorological chart drawn at 1200 GMT on (a) 10 December 1982 and (b) 1 August 1983.

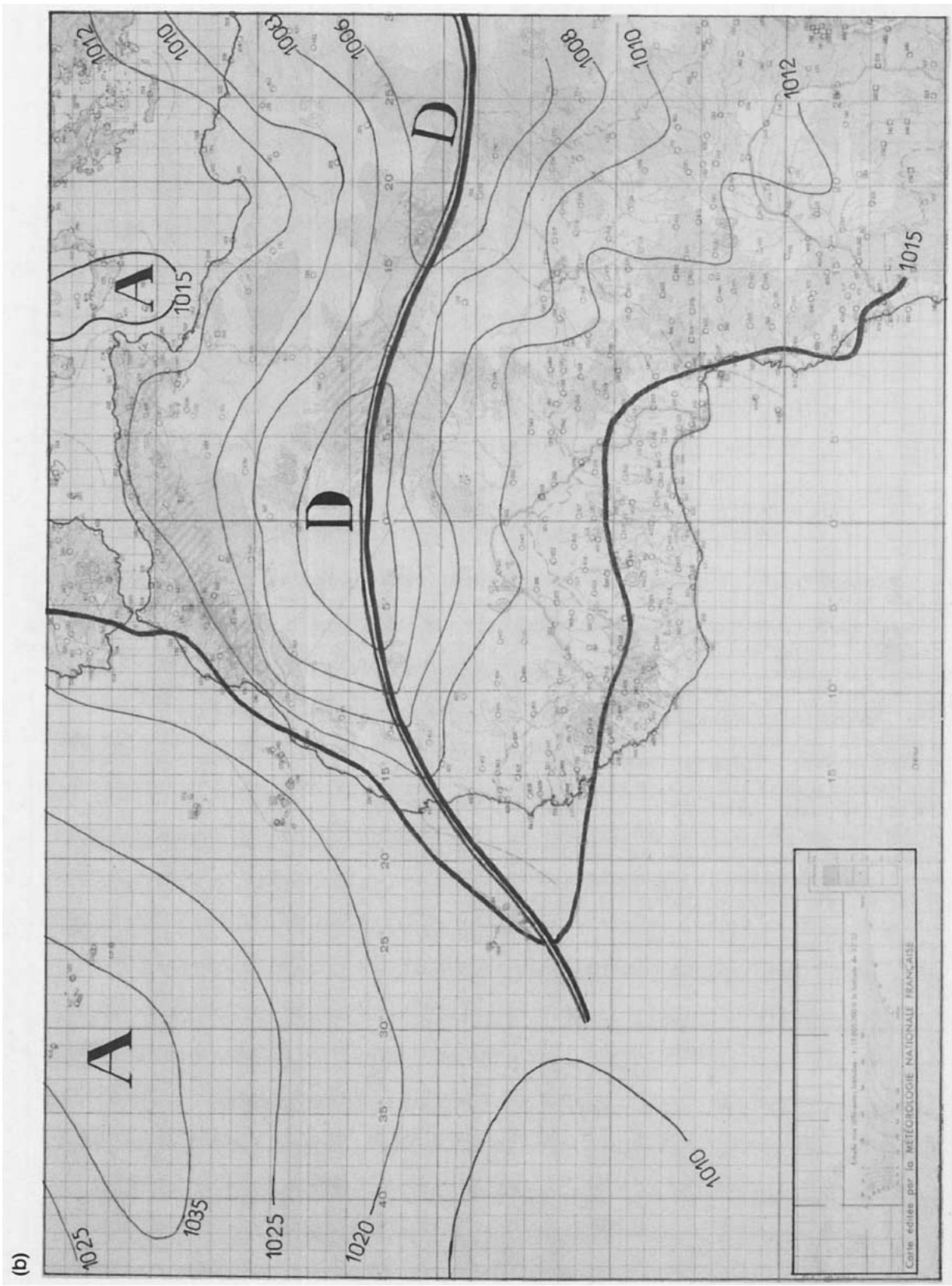

FIG. 5. (*Continued*)

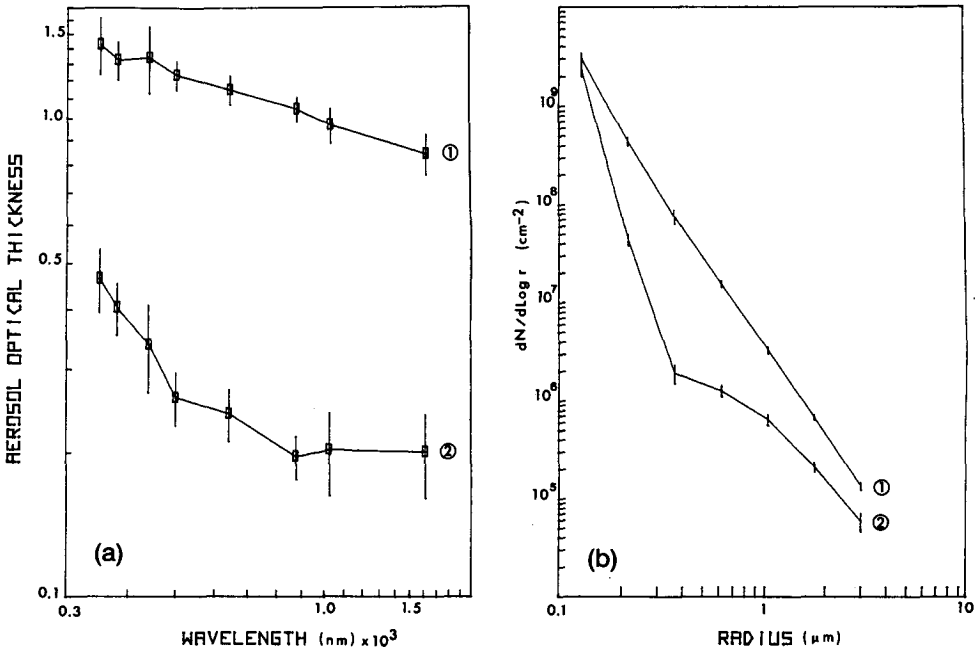

FIG. 6. (a) Plot of spectral aerosol optical thickness versus wavelength: curve 1, 10 December 1982; curve 2, 1 August 1983. (b) Plot of corresponding size distributions vs radius.

Contours of strongly reduced visibilities are also shown; the numbers indicate the surface visibilities in meters. The meteorological conditions at Niamey (NIM on the chart) were the following: visibility, 1 km; wind speed, 5 m s^{-1} from the northeast; relative humidity, 14%; air temperature, 30.5°C; and precipitable water value, w = 1.5 cm. Figure 5b represents a clear (dust free) situation. This chart was drawn at 1200 GMT 1 August 1983, a day with a visibility of 20 km, relative humidity of 58%, air temperature of 31.2°C, wind speed of 2 m s^{-1} from the south, and a precipitable water value of w = 5.1 cm. It should also be noted that it rained the previous day.

Figures 6a, b present the spectral variations of aerosol optical thickness and the corresponding size distribution derived by inversion. Curve 1 on both figures is for measurements performed on 10 December 1982, and curve 2 for 1 August 1983. The radius classes are the following:

Class no.	Radius interval (μm)
1	$0.1 < r < 0.169$
2	$0.169 < r < 0.287$
3	$0.287 < r < 0.486$
4	$0.486 < r < 0.823$
5	$0.823 < r < 1.394$
6	$1.394 < r < 2.361$
7	$2.361 < r < 4.0$

Curve 1 in Fig. 6b compares well with results from measurements performed at the same location under similar meteorological conditions in November 1980 as reported by Cerf et al. (1982). On curve 2 of the same figure one notes high number concentrations in the small size range, although this day was not affected by any dust event. This could indicate that some stratospheric material was present over this region when these measurements were taken.

In order to test the sensitivity to the real physical

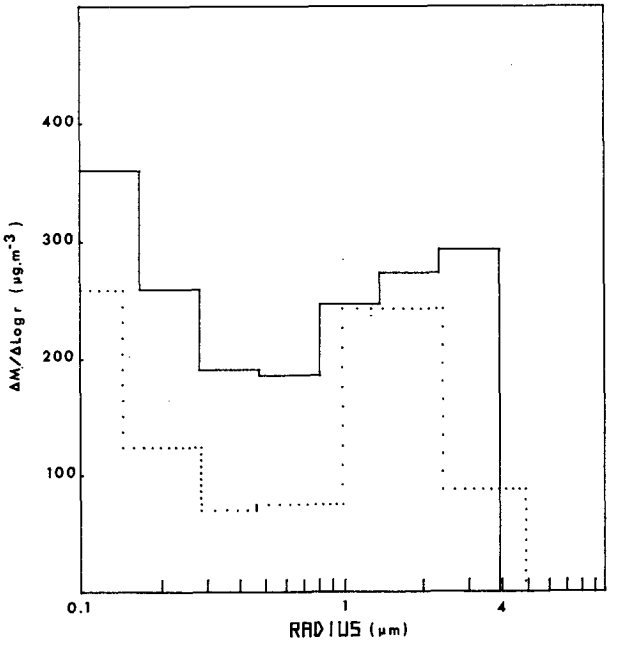

FIG. 7. Plot of mass distribution of airborne soil particles vs radius. Solid line: converted size distribution from inversion of optical data; points: cascade impactor data.

situation of the size distribution retrieval by the inversion method, we converted the size distribution $dN/d \times \log r$ into a "Lundgren-type" mass plot (Lungren et al., 1975), namely, $\Delta M/\Delta \log r$ vs r (in micrometers). The upper cutoff size for stage 1 and the lower cutoff size for stage 6 of the Sierra impactor were given diameter values of 10 and 0.1 μm, respectively. We used a density of 2.6 g cm^{-3}, determined from local soil samples, and a height of Z_i = 1.08 km, determined from soundings. The converted-to-mass-plot size distribution and the impactor mass plot are shown together in Fig. 7, with the solid line representing the converted distribution and the points representing the impactor data. Both the mass sampling and the extinction measurements were carried out on 21 January 1983. The mean visibility and Ångström wavelength exponents were 2 and 0.3 km, respectively.

A direct comparison of the two methods is not entirely valid because the high-volume sampler is in the surface layer and samples for a long time while the inversion integrates quasi-instantaneously along the entire atmospheric path. Nevertheless, the two mass distributions mostly exhibit the same pattern.

7. Conclusion

In this paper the results of measurements of the aerosol optical thickness at eight wavelengths in the 350–1610 nm range, telephotometric spectral horizontal extinction, and airborne particle mass sampling are documented and analyzed together with corresponding surface and upper-air meteorological data.

The relation between spectral aerosol optical thickness and horizontal extinction, as well as between the aerosol optical thickness and surface visibility, has been derived. These results show that the linking parameter between these quantities is the height Z_i, the thickness of the PBL. Thus, it is possible to estimate this height using transmission measurements and visibility observations in remote areas.

The relation between the total mass of airborne soil particles and the horizontal visibility confirms the results obtained in other regions, as well as giving an indication of the size range affecting visibility. These results, together with the similarity between mass distributions derived from the inversion of spectral transmission data and those obtained by classical aerodynamic sampling, strongly support the idea of studying the dust transport over the Sahelian region during the so-called dry season using a combination of a network of multiwavelength transmissometers and satellite observations. Such a program is now being developed.

Acknowledgments. The authors wish to thank the Direction de la Meteorologie Nationale for kindly furnishing the meteorological data used in this study. We also thank Prof. Dr. Jaenicke (University of Mainz) and Prof. Dr. Horvath (University of Vienna) for their help in acquiring the University of Vienna Telephotometer, and Prof. Fouquart and Dr. Bonnel (University of Lille) for their help with the inversion technique.

REFERENCES

Ångström, A., 1929: On the atmospheric transmission of sun radiation and on dust in the air. *Geogr. Ann.*, 156–166.

Ben Mohamed, A., and J.-P. Frangi, 1983: Humidity and turbidity parameters in Sahel: A case study for Niamey (Niger). *J. Climate Appl. Meteor.*, **22**, 1820–1823.

Bertrand, J., J. Baudet and A. Drochon, 1974: Importance des aerosols naturels en Afrique de l'Ouest. *J. Rech. Atmos.*, **8**, 845–860.

Cerf, A., Y. Fouquart, D. Bonnel, G. Brogniez, M. Chaoui-Roquai and L. Smith, 1982: Propriétés radiatives des aerosols saheliens. *La Meteorologie VI^e*, **29**, 247–260.

Charlson, R. J., 1969: Atmospheric visibility related to aerosol mass concentration. *Environ. Sci. Technol.*, **3**, 913–918.

Chepil, W. S., and N. P. Woodruff, 1957: Sedimentary characteristics of dust storms—II. Visibility and dust concentration. *Amer. J. Sci.*, **255**, 104–114.

Deardoff, J. W., 1974: Three-dimensional numerical study of the height and mean structure of heated planetary boundary layer. *Bound.-Layer Meteor.*, **7**, 81–106.

Druilhet, A., J. P. Frangi, D. Guedalia and J. Fontan, 1983: Experimental studies of the turbulence structure parameters of the convective boundary layer. *J. Climate Appl. Meteor.*, **22**, 594–608.

Durand, P., and A. Druilhet, 1982: Contribution à l'étude de la structure turbulente de la couche limite convective Sahelienne en presence de brume sèche. *La Meteorologie VI^e*, **29**, 213–226.

Horvath, H., 1981: The University of Vienna telephotometer. *Atmos. Environ.*, **15**, 2537–2546.

Inn, E. C. Y., and Y. Tanaka, 1953: Absorption coefficient of the ozone in the ultraviolet and visible region. *J. Opt. Soc. Amer.*, **43**, 870–873.

Junge, C. E., 1963: *Air Chemistry and Radioactivity.* Academic Press, 382 pp.

Kaufman, Y. J., and R. S. Fraser, 1983: Light extinction by aerosols during summer air pollution. *J. Climate Appl. Meteor.*, **22**, 1694–1706.

King, M. D., 1982: Sensitivity of constrained linear inversions to the selection of the Lagrange Multiplier. *J. Atmos. Sci.*, **39**, 1356–1369.

——, D. M. Byrne, B. M. Herman and J. A. Reagan, 1978: Aerosol size distributions obtained by inversion of spectral optical depth measurements. *J. Atmos. Sci.*, **35**, 2153–2167.

——, ——, J. A. Reagan and B. M. Herman, 1980: Spectral variations of optical depth at Tucson, Arizona, between August 1975 and December 1977. *J. Appl. Meteor.*, **19**, 723–732.

Lundgren, D. A., and H. J. Paulus, 1975: The mass distribution of large atmospheric pollutants. *J. Air Pollut. Control. Assoc.*, **25**, 1227–1231.

McCartney, E. J., 1976: Optics of the atmosphere. Scattering of the scale height by molecules and particles. Wiley and Sons, 408 pp.

Middleton, W. E. K., 1968: *Vision through the Atmosphere.* University of Toronto Press, 250 pp.

Nicholls, S., and C. J. Readings, 1979: Aircraft observations of the structure of the lower boundary layer over sea. *Quart. J. Roy. Meteor. Soc.*, **105**, 785–802.

Patterson, E. M., and D. A. Gillette, 1977: Measurements of visibility vs mass-concentration for airborne soil particles. *Atmos. Environ.*, **2**, 193–196.

——, ——, and B. H. Stockton, 1977: Complex index of refraction between 300 and 700 nm for Saharan aerosols. *J. Geophys. Res.*, **82**, 3153–3159.

Pendorf, R., 1957: Tables of the refractive index for standard air and the Rayleigh scattering coefficient for the spectral region between 0.2 and 20.0 μm and their application to atmospheric optics. *J. Opt. Soc. Amer.*, **47**, 176–182.

Shaw, G. E., 1973: Investigation of atmospheric extinction using direct solar radiation measurements made with a multiple wavelength radiometer. *J. Appl. Meteor.*, **12**, 374–380.

Tomasi, C, 1982: Features of the scale height for particulate extinction in hazy atmospheres. *J. Appl. Meteor.*, **21**, 931–934.

Volz, F., 1980: *Sky/Sun Photometer Operating Instructions.* Volz, 27 pp.